Universiteit Utrecht

Faculteit Bètawetenschappen

Influence of wind patterns on mass balance and ice sheet evolution during the LGM in North America

Bachelor Thesis

Niels Asberg

Natuur- en Sterrenkunde

Supervisors:

Dr. R.S.W. van de Wal
Institute for Marine and Atmospheric Research Utrecht

Dr. B. de Boer
Institute for Marine and Atmospheric Research Utrecht

June 14, 2017

Abstract

We evaluated the influence of changed wind patterns on the growth of the North American ice sheet during the last glacial, specifically during the Last Glacial Maximum (LGM). For this we simulated the evolution of ice sheets in North America using a 3D ice sheet model (ANICE). Wind was implemented in the model using a two dimensional wind field, either a static Present-Day (PD) wind field or an adjusted wind field, which is an interpolation between a PD wind field and an LGM wind field. The interpolation was based on the global temperature. For the wind fields we used seven different models from the PMIP3 experiment. We also evaluated the use of either 700 hPa or 850 hPa wind fields and compared all our results with a reconstructed geological data-based modelled ice sheet. We found that the PD-wind runs - the runs where only PD wind fields are used - produced a significantly larger LGM ice sheet volume-wise than the adjusted-wind runs, but that their shape and volume was still rather different than those of the comparison ice sheet. The ice sheets from the adjusted-wind runs also differed significantly from the comparison ice sheet, but with suggested adjustments to ANICE's wind implementation these differences might be eliminated. There wasn't much difference in shape between the 700 hPa and the 850 hPa runs, except that at 700 hPa the ice volume was larger on average than at 850 hPa. This larger volume came closer to that of the comparison ice sheet, therefore it looks like using 700 hPa instead of 850 hPa wind fields might work better.

Contents

1 Introduction 1

2 Method 2

2.1 Data 2

2.1.1 PMIP3 experiments 2

2.1.2 Reference ice sheet 3

2.2 Model 3

3 Results 6

3.1 Volume and surface area 6

3.2 Shape 6

4 Conclusion and discussion 11

4.1 Discussion 11

4.2 Conclusion 12

References 13

1 Introduction

During the quaternary period the Earth has been through a number of glacial and interglacial periods. During these glacial periods, the mean temperature of Earth dropped towards the point where continental-scale ice sheets formed, most notably on Eurasia and North America. A big influence is exerted on the shape and growth of these ice sheets by the atmospheric circulation[1]. The wind velocity and direction largely determines where and how much precipitation falls and therefore where the ice sheets grow in size. In turn, the shape of the ice sheets has a large influence on wind patterns, which causes a feedback mechanism.[2]

In this research we examine the influences of changed wind patterns caused by this feedback mechanism on the evolution of ice sheets on North America during the last ice age and specifically during the Last Glacial Maximum (LGM), the point during the last ice age at which the ice sheets were at their largest volume. Here we build on research by B. de Boer *et al.* (2013) [3]. We use the same 3D ice sheet and ice shelf model ANICE, but the model has been modified with a slighty more detailed wind parametrization. In De Boer's research, a static Present Day (PD) wind field was used in combination with orographic forcing - lifting air over rising terrain leading to cooling and precipitation - to calculate precipitation. We will evaluate the difference in using a static PD wind field and an interpolated wind field between PD and LGM wind fields. These wind fields were calculated in seven PMIP3 (Paleoclimate Modelling Intercomparison Project 3) experiments, this is explained in depth in Section 2 "Method". We will also look at the differences between using 850 hPa and 700 hPa wind fields. Usually 850 hPa wind fields are used for such simulations, but because 850 hPa corresponds to a height of about 1.5 km and our ice sheets grow to be over 3 km high, we will also examine 700 hPa wind fields, which correspond to a height of about 3 km.

The wind fields will be interpolated based on the global temperature, which is regarded as an external forcing in this research because we will only simulate North America and not the rest of the world. Therefore the scaling at a certain point in time will be the same for all simulation runs. We will refer to runs that use the interpolation as "adjusted wind" runs, in contrast to the "PD-wind" runs. We will run 28 simulation runs in total. That's 4 for each PMIP3 model: one run with 850 hPa PD-wind, one with 700 hPa PD-wind, one with 850 hPa adjusted wind and finally one with 700 hPa adjusted wind.

2 Method

2.1 Data

2.1.1 PMIP3 experiments

We use wind fields as forcing, originating from seven PMIP3 experiments. PMIP3 means Paleoclimate Modelling Intercomparison Project 3 and is a big project that combines multiple climate models that were all run with the same forcing parameters[4] such as the orbital parameters, concentrations of greenhouse gasses and the land topography. Because climate responses to changes in forcing are largely model dependent[5], such an intercomparison project is key in understanding complex climate processes that require parametrizations. By using the wind fields generated by several different PMIP3 models, we can construct ensembles and averages of the outputs of our simulations.

In Figure 1 some PMIP3 wind fields during the LGM are plotted. CNRM-CM5 and MIROC-ESM are two PMIP3 experiments and their LGM wind fields have the greatest total difference with respect to the seven-model Multi Model Mean (MMM) of all PMIP3 experiments. For illustration, these differences have also been plotted in Figures 1d and 1e.

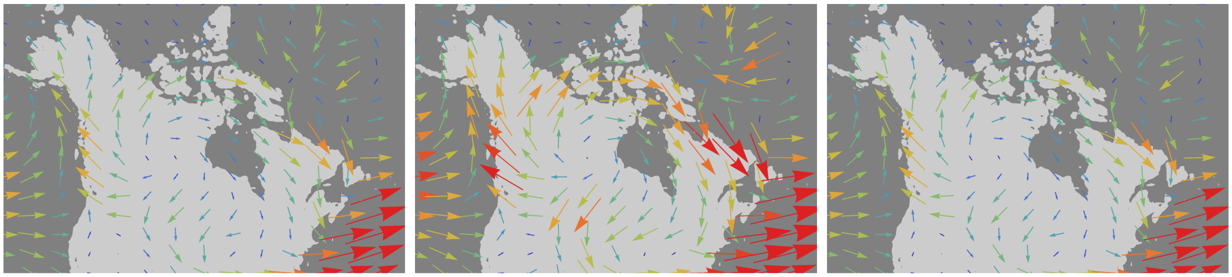

(a) LGM wind, CNRM-CM5 (b) LGM wind, MIROC-ESM (c) LGM wind, MMM

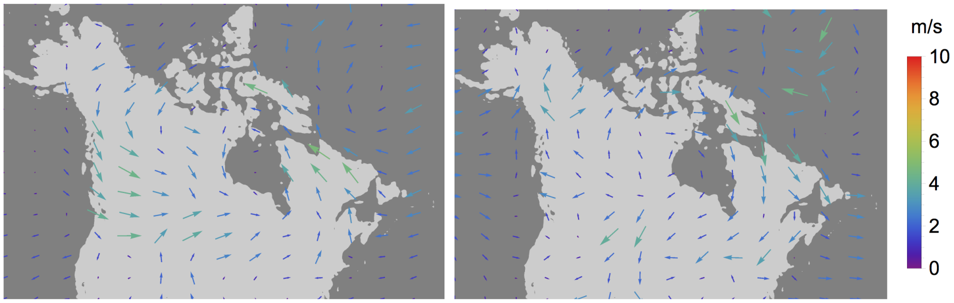

(d) Difference between CNRM-CM5 and MMM LGM wind fields (e) Difference between MIROC-ESM and MMM LGM wind fields

Figure 1: Comparison of wind fields at LGM, we compare the CNRM-CM5 and MIROC-ESM models with the Multi Model Mean (MMM) of the seven PMIP3 experiments. All plots use the same scale.

For present-day (PD) winds I have used data from the same seven PMIP3 experiments, with the addition of ERA40 data. ERA40 is a re-analysis of global climate data originally gathered between 1957 and 2002. The PD wind from ERA40 are the closest we have to the true PD wind because it is based on virtually all recent climate observations.[6] Here we use the mean from 1971 to 2000.

2.1.2 Reference ice sheet

We will compare our results to the results of Tarasov *et al.* (2012)[7], who reconstructed the North American ice sheet at LGM (20 kyr ago) by running a model constrained by geological data. The reason we will use Tarasov's results and not, for example, ICE5-G[8], is that those purely geophysical reconstructions don't take into account matters such as energy conservation and physics of ice deformation. As Tarasov *et al.* put it themselves: "they lack any inherent glaciological self-consistency"[7]. Tarasov used a parametrized surface mass-balance with a shallow ice approximation just as we do with the ANICE model[3]. Their model doesn't directly use wind fields to calculate precipitation as we do (see Section 2.2) but uses a present-day precipitation field which is adjusted with the sea level temperature[9]. For each time step in Tarasov's model each grid point is checked against the constraints set by geological data and if necissary given a correction. The specific 3D ice sheet data set from Tarasov that we will use comes from the run that most closely resembles the mean of the whole ensemble of Tarasov's runs. This ice sheet is plotted in Figure 2b. Next to it, in Figure 2a is the ice sheet that De Boer produced[3], which uses the ANICE model with ERA40 winds.

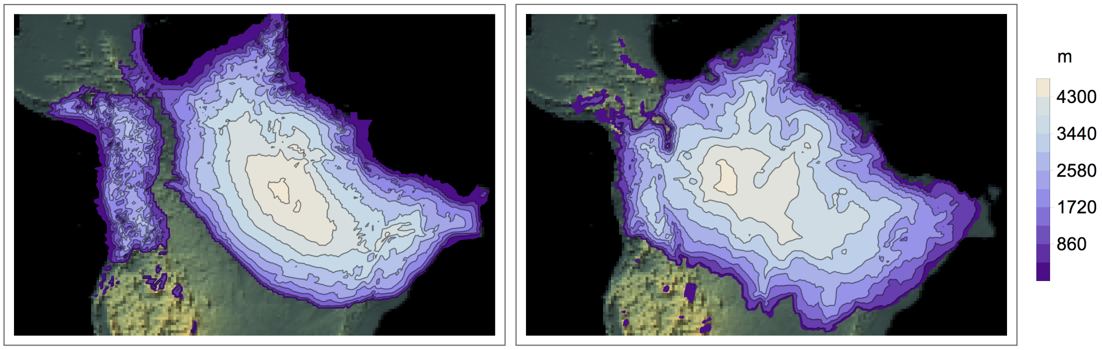

(a) De Boer's ERA40 ice sheet

(b) Tarasov ice sheet

Figure 2: De Boer's and Tarasov's ice sheets at LGM.

In De Boer's ice sheet in Figure 2a an iceless corridor is visible in between the Laurentide ice sheet (the larger eastern sheet) and the Cordilleran ice sheet (the smaller western sheet). This corridor isn't visible in the Tarasov ice sheet in Figure 2b.

2.2 Model

The model used for this research is the IMAU model ANICE, a 3D ice sheet model. This model simulates ice growth over the period of 130 kyr ago to present day. In this section only the parts of this model that are most applicable to this research are presented. For a detailed description of the model we refer you to De Boer *et al.* (2013)[3].

ANICE implements a precipitation model that takes into account orographic forcing and changes in the moisture content. These are calculated from the 2m surface-air temperatures and wind fields.

$$P = e_{\text{sat}}\text{Max}[0, (a + bw_{vv})]f(w_{vv})dw_{vv} \tag{1}$$

The saturation vapour pressure e_{sat} (mbar) is related to the moisture content of the atmosphere given by the Clausius-Clapeyron relation as a function of the surface-air temperature in °C:

$$e_{\text{sat}} = e_0 e^{c_1 \frac{T_s}{c2+T_s}} \tag{2}$$

Where $e_0 = 6.112\,\text{mbar}$ is the reference saturation vapour pressure, $c_1 = 17.67$ and $c_2 = 243.5\,°\text{C}$ the Clausius-Clapeyron parameters.[3] The vertical uplift is controlled by the two parameters a and b in Equation 1 that define the background precipitation rate and the influence of the vertical velocity, respectively: $a = 2.5 \times 10^{-11}\,\text{m}^2\,\text{s}\,\text{kg}^{-1}$ and $b = 5.9 \times 10^{-9}\,\text{m}\,\text{s}^2\,\text{kg}^{-1}$.

The vertical velocity w_{vv} is defined using the horizontal winds and surface slope:

$$w_{vv} = \text{Max}[0, v_x \frac{\partial H_s}{\partial x} + v_y \frac{\partial H_s}{\partial y}] \tag{3}$$

Here H_s is the surface elevation and v_x and v_y are the x and y components of a wind field interpolated for the ice-sheet grid. Finally, The function $f(w_{vv})$ from equation 1 is a Gaussian probability distribution function of w_{vv}:

$$f(w_{vv}) = \frac{e^{-(\frac{wvv - wvv,0}{a_{vv}})^2}}{N} \tag{4}$$

Where N is a normalisation factor and a_{vv} is a measure for the variability of the vertical velocity. The uplift is spatially variable and introducing this distribution function takes care of that.

In some parts of this research we use adjusted wind fields where the wind field components v_x and v_y are linearly interpolated between an LGM and a PD wind field:

$$v_i = sv_{i,\text{LGM}} + (1 - s)v_{i,\text{PD}} \tag{5}$$

where s is the scale factor, defined as

$$s = \text{Min}[1, \text{Max}[0, \frac{\Delta T}{-15}]] \tag{6}$$

Where ΔT is the global temperature difference relative to PD. Here the temperature difference at the LGM is assumed to be $-15\,°\text{C}$ and ΔT is therefore clamped between $0\,°\text{C}$ and $-15\,°\text{C}$. The ΔT data was calculated with a global ANICE run by De Boer *et al.* (2013)[3] which included all ice sheets. This data is shown below in Figure 3 together with the scale factor over time.

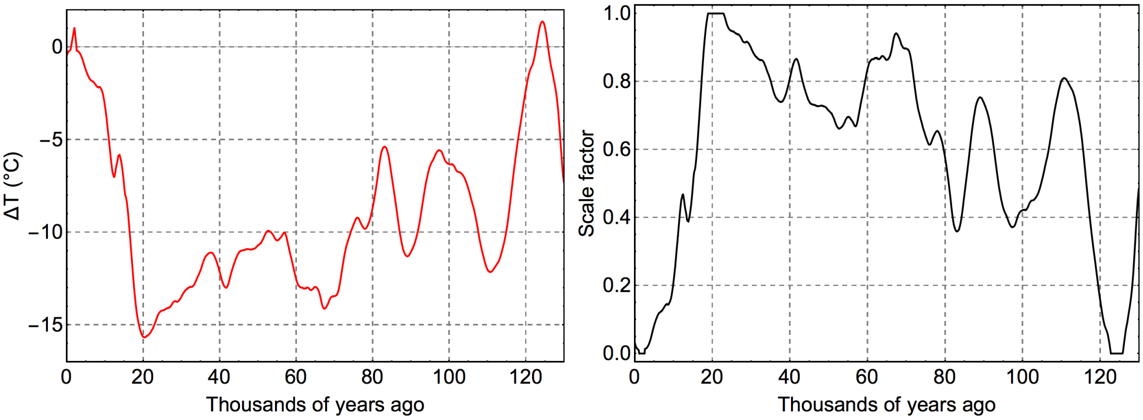

(a) The temperature difference ΔT over time (b) The scale factor s over time

Figure 3: The temperature difference ΔT data and derived scale factor as in Equation 6 over time.

3 Results

3.1 Volume and surface area

In this section we compare the volumes and surface areas of our results with the measurement-based LGM ice sheet at 20 kyr ago reconstructed by Tarasov *et al* (2012)[7] as discussed in Section 2.1.2, to which we will refer as the Tarasov ice sheet. In Figure 4a the land ice volume in mESL (meters eustatic sea level equivalent) is plotted for all model runs at 700 hPa, with adjusted wind (purple) and with PD-wind (green). The same in Figure 4b but with 850 hPa, with adjusted wind (blue) and with PD-wind (red). For reference there's also the black dashed line representing the ERA40 850 hPa wind field simulation, and the orange data point representing the mESL of the Tarasov ice sheet at 20 kyr ago, namely 70.1 ± 2 mESL [7].

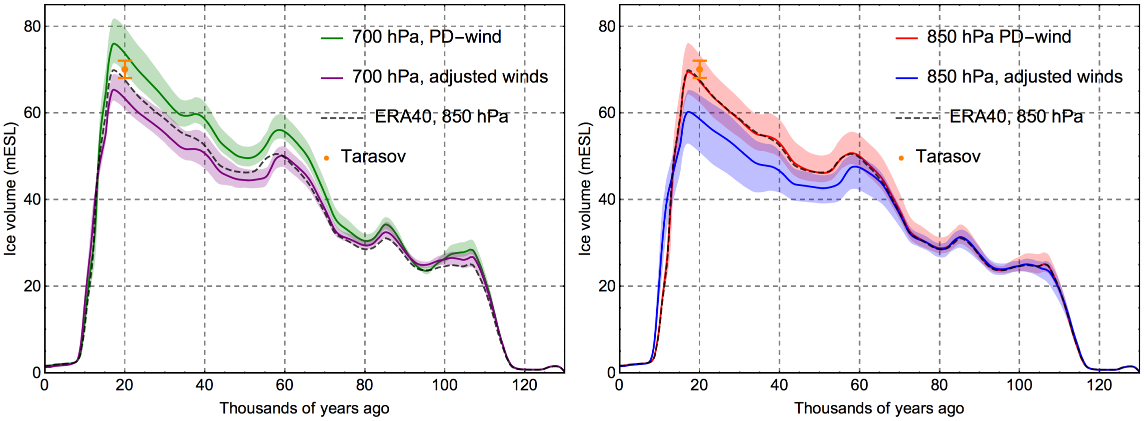

(a) 700 hPa land ice volume (b) 850 hPa land ice volume

Figure 4: The land ice volume for 700 and 850 hPa runs, with PD-wind and with adjusted wind. The green and red spreads are the PD-wind runs, with the green and red lines the mean values at each time step. The purple and blue spreads and lines are the data with adjusted wind. The dashed black line is the data from a run with only the ERA40 850 hPa wind field which is the wind field De Boer *et al.* (2013) used[3] in their simulations. Finally, the orange data point is the volume in mESL of the Tarasov ice sheet at 20 kyr ago, 70.1 ± 2 mESL[7]

In Figure 4 the Tarasov ice sheet volume lies within the 700 hPa PD-wind runs and partly within the 850 hPa PD-wind runs. Also, you can see that the ERA40 simulation closely follows the PD-wind mean land ice volume curve at 850 hPa. This is a good sign, it means that the effects of the present day winds of the PMIP3 models average out to the best known present day wind field. Generally the PD-wind simulations have a bigger volume, about 10 - 20 % more at LGM compared to the simulations with adjusted wind.

3.2 Shape

The simulations start really diverging around 70 kyr ago in Figure 4, this correlates with the time the Laurentide (eastern) and Cordilleran (western) ice sheets start merging in the runs with adjusted wind, but not quite (yet) in the PD-wind runs as you can see in Figure 5.

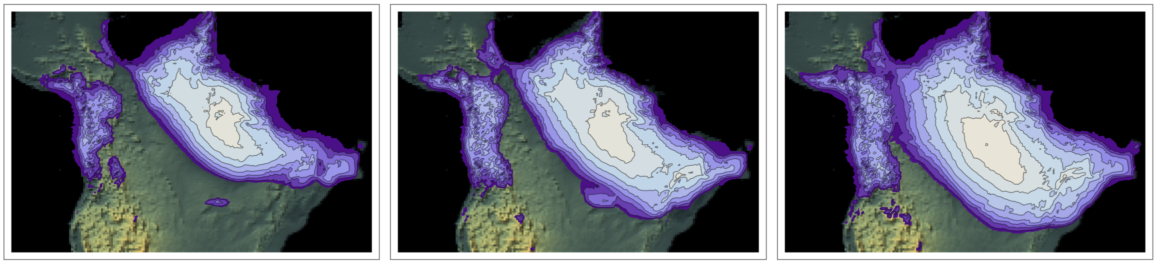

(a) 850 hPa PD-wind, 70 kyr ago (b) 850 hPa PD-wind, 60 kyr ago (c) 850 hPa PD-wind, LGM (17 kyr ago)

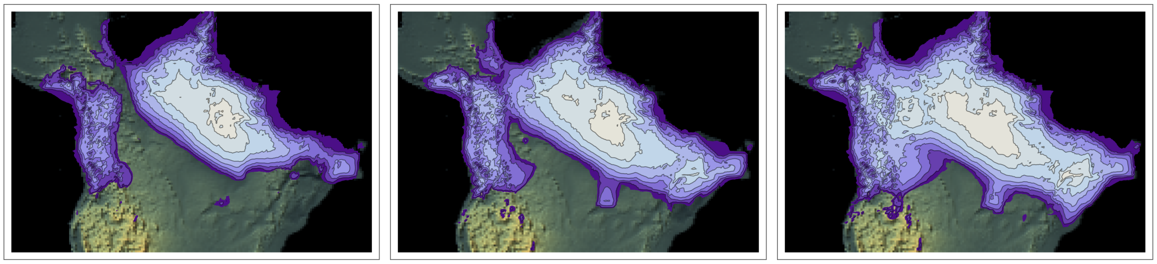

(d) 850 hPa adjusted, 70 kyr ago (e) 850 hPa adjusted, 60 kyr ago (f) 850 hPa adjusted, LGM (17 kyr ago)

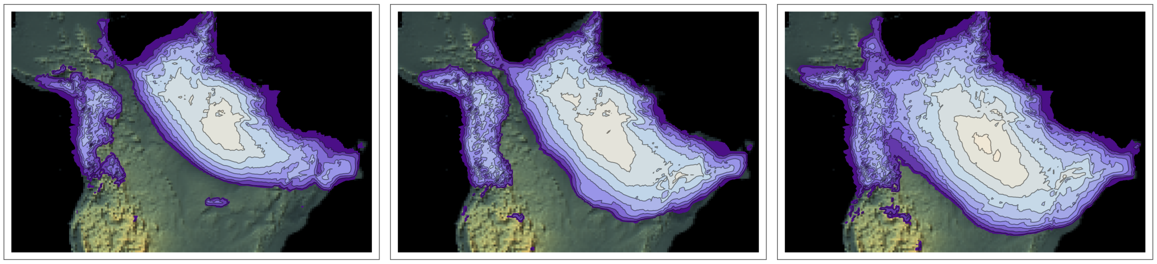

(g) 700 hPa PD-wind, 70 kyr ago (h) 700 hPa PD-wind, 60 kyr ago (i) 700 hPa PD-wind, LGM (17 kyr ago)

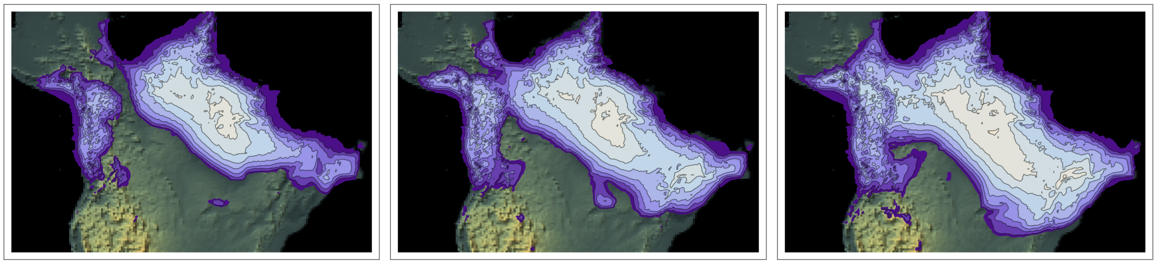

(j) 700 hPa adjusted, 70 kyr ago (k) 700 hPa adjusted, 60 kyr ago (l) 700 hPa adjusted, LGM (17 kyr ago)

Figure 5: Comparison of the average ice sheets (averaged over model runs) at 70 kyr ago, 60 kyr ago and at LGM (17 kyr ago). It shows that the runs with adjusted wind close the ice-free corridor in between the Laurentide (eastern) and Cordilleran (western) ice caps between 60 and 70 kyr ago, which isn't true for the PD-wind runs. The scale in these images is the same as in Figure 2.

Around this period, so 70 to 60 kyr ago, the scale factor from Equation 6 is around 0.85 to 0.90, which indicates that the wind at this point in time consists mostly of the LGM wind field. This is shown as example with the IPSL-CM5A-LR model's winds in Figure 6. The wind together with the ice sheet at 60 kyr ago is shown in Figure 7. That the merging of the ice sheets causes the ice volume to increase more rapidly (see Figure 4) can be attributed to the fact that when the Laurentide and Cordilleran ice sheets join, the new edge of the ice stands perpendicular to the wind field at that point. This causes the vertical wind velocity to increase, which in turn causes the amount of precipitation to increase as well, as in Equation 1, which results in faster ice growth. With the same reasoning we can see that the eastern winds at the southernmost point of the Laurentide ice sheet causes that ice sheet to grow slightly towards the west. It's also what causes the 'belly' of the Laurentide ice sheet to grow further towards the south in the PD-wind simulations. In runs with adjusted wind the winds point away from the ice sheet in that location as in Figure 7, but they point slightly towards it in the PD wind fields.

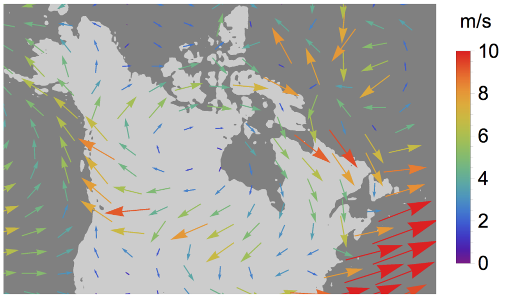

(a) IPSL 850 hPa wind at LGM

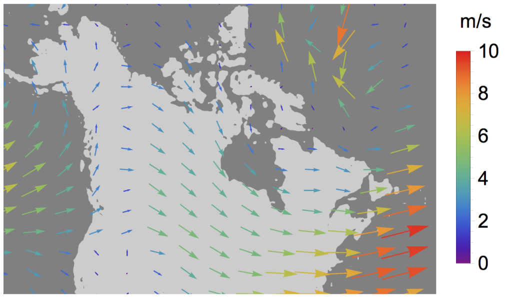

(b) IPSL 850 hPa wind at PD

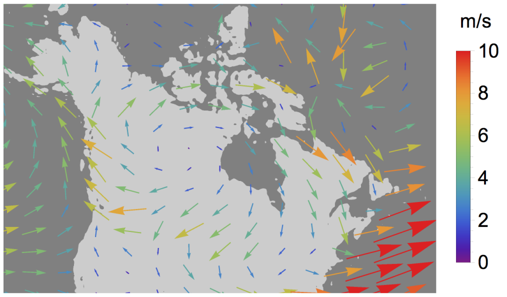

(c) IPSL 850 hPa wind at 65 kyr ago

Figure 6: The IPSL-CM5A-LR 850 hPa wind fields at LGM, PD and 65 kyr ago.

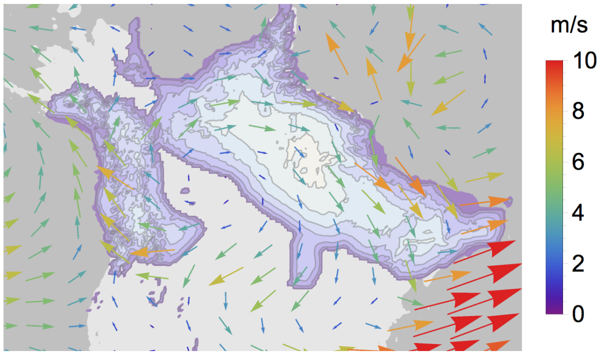

Figure 7: 850 hPa adjusted wind IPSL-CM5A-LR ice sheet at 60 kyr ago along with the wind at that point. Here $\Delta T = -12.6°C$ and the scale factor $s = 0.84$.

In Figure 8a the volume overlap difference is plotted for each type of wind field (700 and 850 hPa, with PD-wind and with adjusted wind) with respect to the Tarasov ice sheet. The same for Figure 8b but with surface area.

A positive difference in Figure 8 indicates that there is ice in places where there is none or less in the Tarasov ice sheet, a negative difference indicates that there is no or less ice in places compared to the Tarasov ice sheet. The differences were calculated for each grid point and added together, for this we interpolated the Tarasov ice sheet from its 1° × 0.5° grid[7] to our 40km × 40km grid.

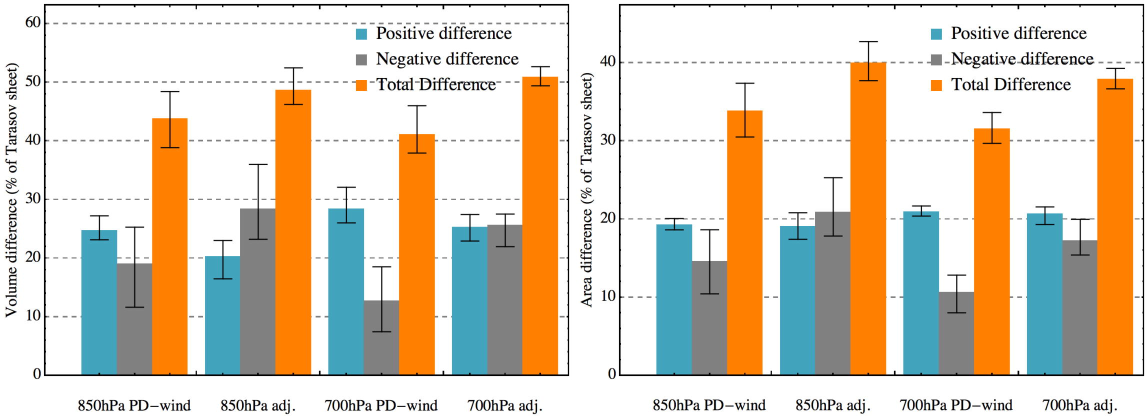

(a) Land ice volume difference

(b) Land ice area difference

Figure 8: Differences between the Tarasov ice sheet at its LGM (20 kyr ago) and the simulated ice sheets from this research at its LGM (17 kyr ago). The blue bars indicate a positive difference: the amount of ice there is in different places than in the Tarasov ice sheet. The gray bars indicate a negative difference: the amount of ice that is present in the Tarasov ice sheet in places that there is no or less ice in our simulation runs. The orange bars indicate the total difference, so positive + negative for each run.

The 700 hPa PD-wind runs have the lowest average total difference, closely followed by the 850 hPa PD-wind runs, for both volume and area comparisons. All ice sheets differ significantly form the Tarasov ice sheet. The differences for averages of runs lie between 41% and 51% for volume and between 31% and 40% for surface area.

The ice sheets from all simulations are shown in Figure 9. In some simulations an iceless corridor is still visible at LGM in between the Laurentide and Cordilleran ice sheets. The corridor is uninterrupted only with the PD-wind 850 hPa IPSL-CM5A-LR and MPI-ESM-P runs. It's also still distinctly visible although not completely ice free at some other PD-wind runs, both with 850 hPa and 700 hPa wind fields. In runs with adjusted wind the iceless corridor disappears completely as discussed earlier, but it makes place for a bigger gap in the ice sheet around the great plains in the middle of the continent.

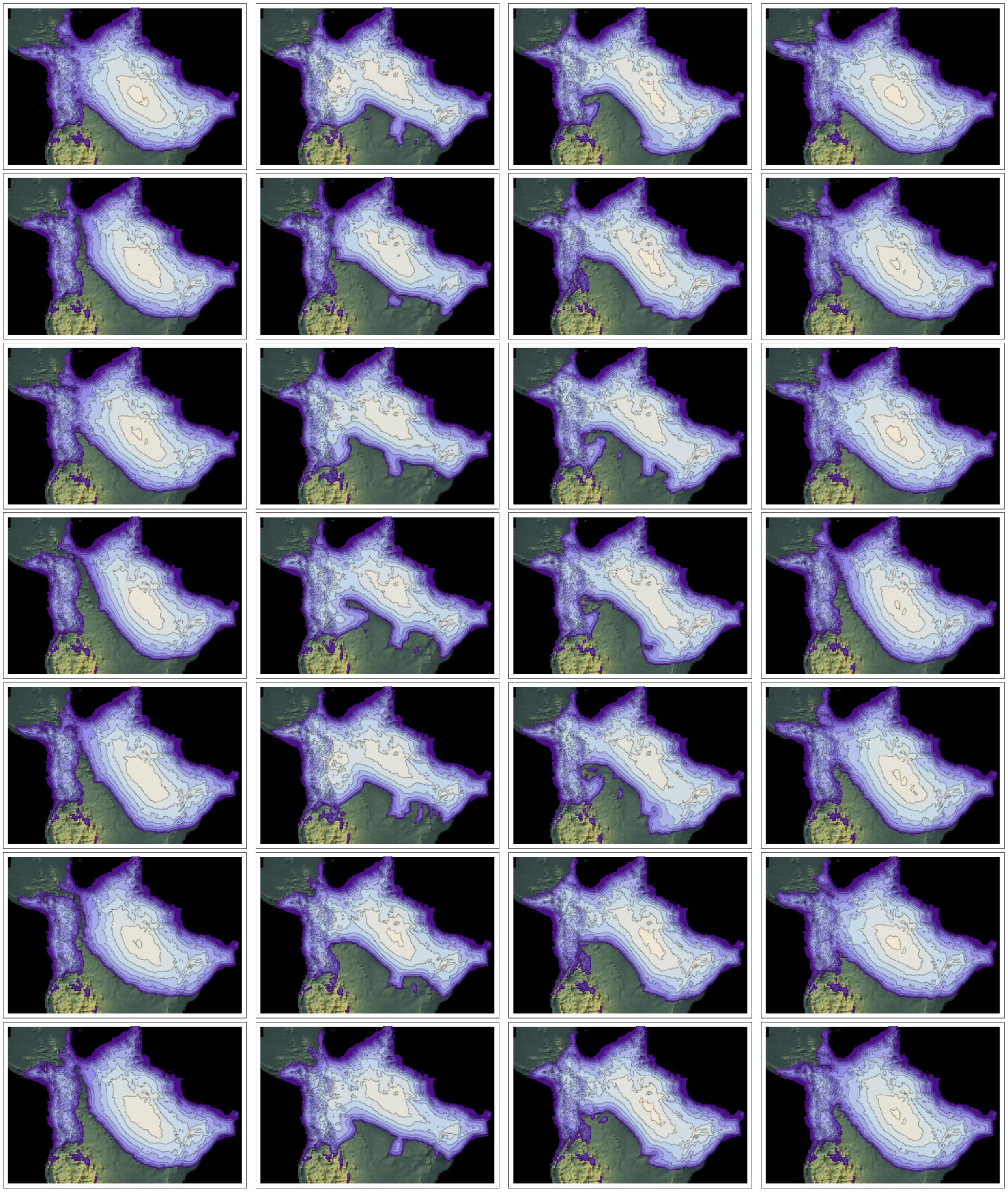

(a) 850 hPa, PD-wind

(b) 850 hPa, adjusted wind

(c) 700 hPa, adjusted wind

(d) 700 hPa, PD-wind

Figure 9: Visual plots of the ice sheet at LGM, one model per row. From top to bottom: CCSM4, CNRM-CM5, FGOALS-s2, IPSL-CM5A-LR, MIROC-ESM, MPI-ESM-P, MRI-CGCM3. The scale in these images is the same as in Figure 2.

4 Conclusion and discussion

4.1 Discussion

The shape of the North American ice sheet used in the PMIP3 experiments to simulate the wind fields at LGM[10], as shown in Figure 10, is very different than the ice sheets simulated with ANICE in this experiment. Therefore even at LGM the wind fields don't fully reflect the influence of the specific shape of our ice sheet.

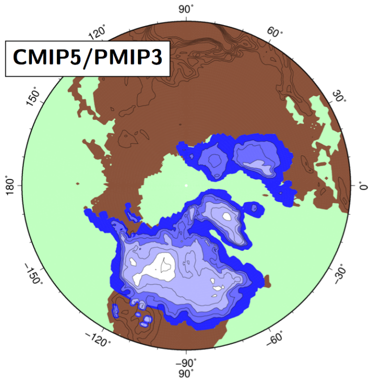

Figure 10: Northern hemisphere ice sheets as used in the PMIP3 experiments, from Abe-Ouchi *et al.* (2015)[10]

When using the adjusted wind fields, we scaled between PD and LGM winds using the global temperature, but this isn't the only parameter we could use for this. It might also be considered to scale using for example the ice volume or surface area as these parameters also reflect the transition from PD to LGM conditions. If you compare for example Figures 4 and 3 you can see that the temperature data approaches LGM values more quickly than the volume data. So if you were to use volume instead of temperature as the scaling parameter, the PD wind would have a larger contribution to the wind field on average which might cause the southern part of the Laurentide ice sheet to join with the Cordilleran ice sheet and fully close the gap in between them, as discussed on page 8.

Of course, the way we have implemented wind in our simulation is very simple. A different more complex algorithm might give results that come closer to the Tarasov ice sheet if it can implement more aspects of the feedback mechanism between ice sheet and wind, ideally by directly simulating wind interaction with the 3D ice sheet in some way. Our simulation is fairly quick to run, one run takes about one to two hours on a modern personal computer and on multicore machines multiple simulations can be run at the same time. So there is definitely room for a more complex algorithm to be run in a reasonable amount of time.

Finally, the Tarasov ice sheet we used to compare our results to isn't the only option for this. There are plenty other ice sheet models that have differing results, and there are others that could also be considered for this. But as I argued in Section 2.1.2, the Tarasov ice sheet reconstruction seems to be the best option we have at this time because it combines a 3D ice sheet model with geophysical constraints and is therefore both physically self-consistent and consistent with measured geophysical data. Another option we considered, the ICE5-G reconstruction[8], is consistent with measured geophysical data but isn't glaciologically self-consistent[7].

4.2 Conclusion

Although adjusting the wind fields by scaling by temperature between PD and LGM winds implements a more responsive parametrisation than just using the PD winds, it doesn't necissarily help our ice sheet to grow into the same shape and size as our reference Tarasov ice sheet. If we just look at land ice volume, only the 850 hPa PD-wind runs and 700 hPa PD-wind runs actually match with the Tarasov ice sheet volume data point. Just within its uncertainty, the Tarasov ice sheet volume also has a small overlap with the 700 hPa runs with adjusted wind. This seems to indicate that, volume-wise, using 700 hPa wind fields might work out better than using 850 hPa wind fields.

As for the shape of the ice sheet during LGM, the PD-wind runs still have either an ice-free corridor between the Laurentide and Cordilleran ice sheets or a very obvious remnant of it, as seen in Figure 9. According to Dyke *et al.* (2002)[11] the ice-free corridor closed at least partly during LGM, there is evidence for this particularly in the southern part of the corridor. The southern extent of the PD-wind runs is about the same as the Tarasov ice sheet, see Figure 11. But the peak of the ice sheet is in a different place, it's more towards the west compared to that of the Tarasov ice sheet. As for the adjusted wind runs, they don't have the corridor at LGM, except for a small remnant in the 850 hPa CNRM-CM5 run (see Figure 9). They don't extend as far south as the Tarasov ice sheet.

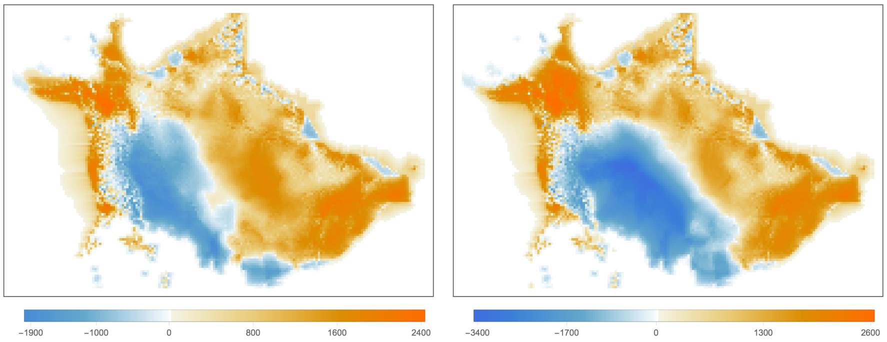

(a) 700 hPa PD-wind (b) 700 hPa adjusted wind

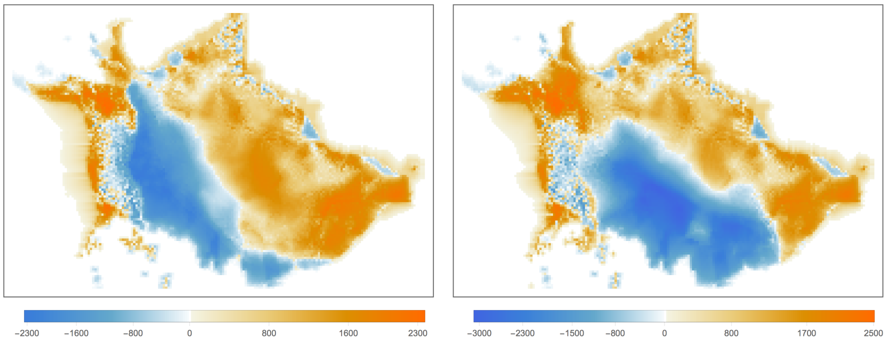

(c) 850 hPa PD-wind (d) 850 hPa adjusted wind

Figure 11: Difference plots between the averaged ice sheets from Figure 5 and the Tarasov ice sheet. Blue colors indicate where the Tarasov ice sheet is thicker, orange colors indicate where our ice sheet is thicker.

But we also have to take into account the difference plots in Figure 8. Here we see that, both for volume and area, the 700 hPa PD-wind runs have the smallest difference to the Tarasov ice sheet, closely followed by the 850 hPa PD-wind runs. So looking at this shape difference, it's hard to immediately tell which approach is better.

Based on the volume and area data combined with the arguments we gave in Section 4.1 about possible adjustments to the implementation of wind in the ANICE model, we can conclude that the wind adjustment introduced in this research has potential to improve the results of the ANICE model towards the point that its output ice sheet resembles the Tarasov ice sheet more. It also looks like using 700 hPa wind fields instead of 850 hPa wind fields might work better.

References

[1] G. H. Roe and R. S. Lindzen, Climate Dynamics **17**, 479 (2001).

[2] P. Beghin, S. Charbit, C. Dumas, M. Kageyama, D. M. Roche, and C. Ritz, Climate of the Past **10**, 345 (2014).

[3] B. de Boer, R. S. W. van de Wal, L. J. Lourens, R. Bintanja, and T. J. Reerink, Climate Dynamics **41**, 1365 (2013).

[4] T. Sueyoshi, R. Ohgaito, A. Yamamoto, M. O. Chikamoto, T. Hajima, H. Okajima, M. Yoshimori, M. Abe, R. O'ishi, F. Saito, et al., Geoscientific Model Development **6**, 819 (2013).

[5] P. Braconnot, B. Otto-Bliesner, S. Harrison, S. Joussaume, J.-Y. Peterchmitt, A. Abe-Ouchi, M. Crucifix, E. Driesschaert, T. Fichefet, C. D. Hewitt, et al., Climate of the Past **3**, 261 (2007).

[6] S. Uppala, P. Kållberg, A. Simmons, U. Andrae, V. da Costa Bechtold, M. Fiorino, J. Gibson, J. Haseler, A. Hernandez, G. Kelly, et al., Quart. J. Roy. Meteor. Soc. **131**, 2961 (2005).

[7] L. Tarasov, A. S. Dyke, R. M. Neal, and W. Peltier, Earth and Planetary Science Letters **315316**, 30 (2012).

[8] W. Peltier, Annual Review of Earth and Planetary Sciences **32**, 111 (2004).

[9] L. Tarasov and W. R. Peltier, Journal of Geophysical Research: Atmospheres **104**, 9517 (1999).

[10] A. Abe-Ouchi, F. Saito, M. Kageyama, P. Braconnot, S. P. Harrison, K. Lambeck, B. L. Otto-Bliesner, W. R. Peltier, L. Tarasov, J.-Y. Peterschmitt, et al., Geoscientific Model Development **8**, 3621 (2015).

[11] A. Dyke, J. Andrews, P. Clark, J. England, G. Miller, J. Shaw, and J. Veillette, Quaternary Science Reviews **21**, 9 (2002).